JULY 2010 VOLUME 22 NUMBER 7

PHYSICS OF FLUIDS

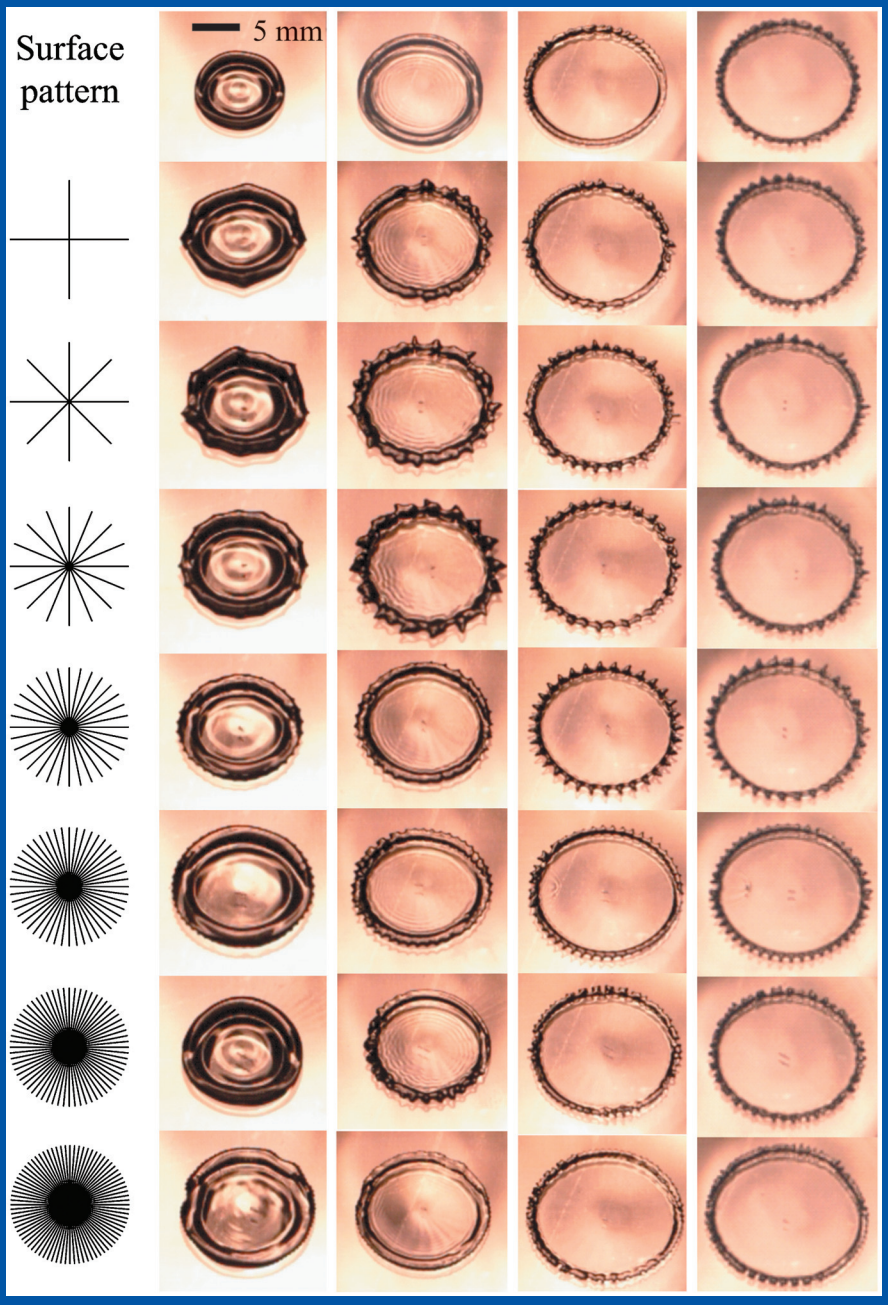

AIP

Drop impact on microwetting patterned surfaces

Minhee Lee,[1] Young Soo Chang,[2] and Ho-Young Kim[1,a)]
[1]*School of Mechanical and Aerospace Engineering, Seoul National University, Seoul 151-744, South Korea*
[2]*Department of Advanced Fermentation Fusion Science and Technology, Kookmin University, Seoul 136-702, South Korea*

(Received 12 February 2010; accepted 10 June 2010; published online 15 July 2010)

We investigate experimentally the dynamics of a liquid drop that impacts on a solid surface whose wettability is patterned at the microscopic scale. The target surface is patterned such that hydrophilic (hydrophobic) microscale spokes radiate from the center on a hydrophobic (hydrophilic) background. Following the initial spreading stages, the drop recoils on the hydrophobic region while being arrested on the hydrophilic area, thereby resulting in a micropatterned liquid footprint. We also find that the fingering instability of the drop edge is affected by the wettability patterns in the initial spreading stages. The number of fingers depends on a combination of the impact Weber number and the number of spokes. We suggest that the present scheme of patterning liquid deposits at microscales could be exploited in various microfluidic applications. © *2010 American Institute of Physics*. [doi:10.1063/1.3460353]

I. INTRODUCTION

The behavior of a liquid drop upon collision with a solid surface has been the subject of intense study for more than a century.[1–3] The study of drop impacts on solids is important in understanding natural phenomena involving raindrops and in many technical applications including ink-jet printing, spray coating,[4] spray cooling,[5] and solder jet bumping.[6] For fixed impact conditions (e.g., size, velocity, and material of the liquid drop), the physical and chemical characters of the target surface determine the drop dynamics. The dynamics generally consists of an initial spreading phase, followed by recoiling. On the one hand, a water drop impacting on a hydrophobic surface exhibits a vigorous oscillation.[7] On the other hand, an identical impact onto a hydrophilic surface causes the drop to spread into a thin lenslike shape with negligible oscillations.[8] Coordinating the vertical motion of the target surface with the impinging drop was shown to control the degree of drop rebound.[9] When a water drop hits a superhydrophobic surface with a low contact angle hysteresis, it bounces like an elastic ball.[10] A drop impacting with a high inertia splashes or develops fingers around its rim,[11] and such instability is reported to be amplified on rough surfaces.[12] These findings suggest that the drop impact behavior can be tailored to an extent by controlling the physicochemical properties and dynamic states of the solid surface.

Thanks to recent developments in micro- and nanofabrication technology, it is possible to create a variety of surfaces with tailored wettability and physical morphology. Among those surfaces, superhydrophobic surfaces have been used by many researchers to show that the drops are strongly repelled by the surfaces upon impact.[10,13,14] On wettable micropillar arrays, the shape of a drop was shown to deviate from that of an axisymmetric lens depending on the pillar wettability, distribution, and dimensions,[15–18] but their effect on impact dynamics was not addressed. Drop impact onto microfabricated rough surfaces was studied to show the effects of the surface texture patterns in guiding liquid flow and promoting splashes.[19–21] Unlike previous studies, which mainly relied on surface *topography* to control drop impact behavior and postdeposition shapes, here we show that the micropatterning of *wettability* of the target surface gives rise to the shape evolution of a drop and the final deposit shape that are novel and even aesthetically pleasing.

Microscale patterns of wettability have previously been used to guide a liquid flow without resorting to physical walls of microchannels. Kataoka and Troian[22] produced flow along thin hydrophilic lines driven by thermocapillary effects, while the neighboring hydrophobic region remained dry. Zhao *et al.*[23] used hydrophilic lanes formed inside microchannels as virtual conduits for microliquid streams. The liquid flows in those studies were driven by capillary forces with negligible effect of inertia. In contrast, the current study concerns flow that is initially driven by high impact inertia. Upon drop impact, the liquid initially spreads both on the wettable and nonwettable areas until its kinetic energy is largely converted into surface energy and viscous dissipation. Then the liquid on hydrophobic regions retracts, while the liquid is arrested on hydrophilic areas. Although not as dramatic as the recoiling process, the initial spreading stages are also shown to be affected by the wettability patterns: the fingering instability of the spreading rim is provoked by the patterns. In this paper, we visualize and quantify these drop motions.

II. MATERIALS AND METHODS

To selectively pattern the wettability of a solid surface, we begin with a glass surface cleaned with piranha solution, which turns the glass perfectly wettable by water. A schematic of the subsequent procedures is shown in Fig. 1: a positive photoresist (AZ1512) is spin-coated on the glass

a)Author to whom correspondence should be addressed. Electronic mail: hyk@snu.ac.kr. Telephone: 82-2-880-9286. Fax: 82-2-880-9287.

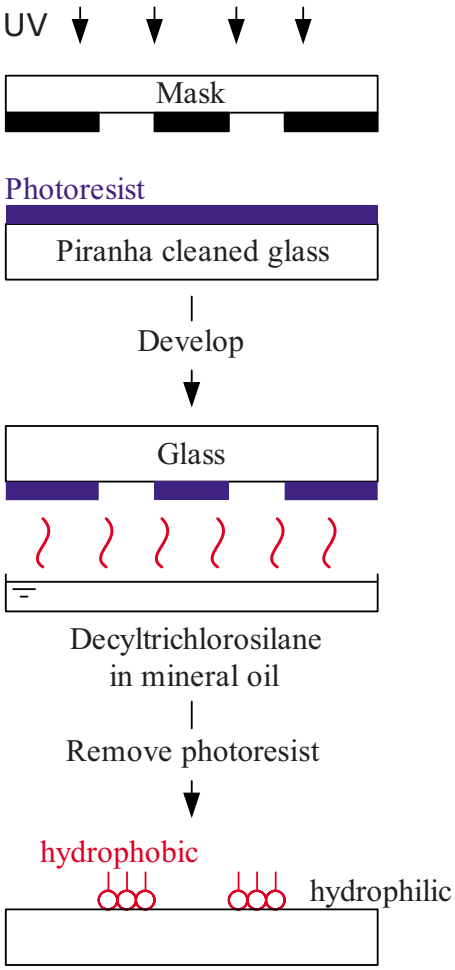

FIG. 1. (Color online) The process of the surface wettability patterning.

surface at 500 rpm for 5 s and then at 3500 rpm for 35 s. It is then baked on a hot plate at 100 °C for 5 min. Ultraviolet (UV) exposure is carried out with a dose of 265 W m^{-2} for 11 s with a photomask on the photoresist-coated glass. After removing the irradiated photoresist with a developer, the photoresist-patterned glass surface is exposed to the vapor of a solution of mineral oil and decyltrichlorosilane, $Cl_3Si(CH_2)_9CH_3$, with the weight ratio (oil:silane) of 7:5, for 3 min. Through this step, the exposed glass surface is coated with a hydrophobic self-assembled monolayer (SAM).[24] Finally, removing the residual photoresist with acetone for 20 s exposes the original hydrophilic regions. We are thus left with a glass surface with wettability patterns: hydrophobic in regions coated with SAM and hydrophilic elsewhere. The equilibrium contact angle of de-ionized water on glass coated with the silane SAM is measured to be 105° and that on a piranha cleaned surface is 3°. The critical advancing and receding contact angles for the silane SAM are measured to be 106° and 84°, respectively, and those for the piranha cleaned surface are 4° and 2°, respectively. The qualities of the wettability pattern, i.e., the contrast of the contact angles on the hydrophobic and the hydrophilic regions and the durability of the self-assembled monolayer, depend on the mixing ratio of the oil-silane solution, the exposure time to the

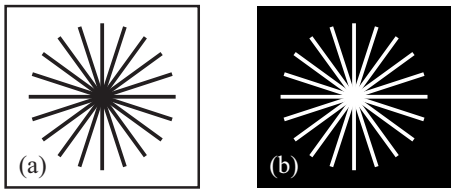

FIG. 2. Two representative mask patterns used for vertical drop impact leading to surface patterns with radiating thin spokes that are (a) hydrophilic and (b) hydrophobic.

diffusing vapor, and the acetone cleansing time, all of which were optimized through repetitive tests.

Figure 2 shows the representative photomask patterns which radiate thin spokes from the center. The patterns formed along such a flow direction have been found to exert the most significant influence on the drop dynamics compared to other patterns tested including concentric circles, parallel lines, and square grids of alternating wettability. This is because the drop spreads and recoils in the radial direction. On the target surface, the area corresponding to the dark photomask region remains hydrophilic, while the transparent photomask area results in a hydrophobic region. The number and the thickness of radiating spokes were varied to investigate their effects on the drop spreading behavior.

We use de-ionized water emitting from a micropipette to create liquid drops of radius $R=1.65$ mm. They fall under gravity to impact on a horizontal solid surface. The impact velocity of a drop U is varied by changing the distance it travels. The shape evolution of the drop is recorded by a high-speed camera (Redlake HS4-C-2) at a rate of 5000 frames/s with the pixel resolution of 436×416.

III. RESULTS AND DISCUSSION

A. Generic dynamics of spreading and recoiling

To introduce the generic effects of the wettability patterns on the drop impact dynamics, we show in Fig. 3 sequences of images of a water drop colliding with a highly wettable glass, the silane SAM surface, a surface with hydrophilic spokes corresponding to the photomask pattern of Fig. 2(a), and a surface with hydrophobic spokes corresponding to the mask of Fig. 2(b). In each of these cases, the impact velocity of the drops is 2.8 m/s, so that the impact Weber number defined as $We=\rho U^2R/\sigma$, where ρ and σ is the density and the surface tension of the liquid, respectively, is We=186. All four drops spread to resemble a thin disk with a bulging rim in the initial spreading stages. At this stage, the only discernible difference is that tiny corrugations start to develop in the rims of the drops of Figs. 3(c) and 3(d). The effects of the surface wettability manifest themselves very clearly in the recoiling stages, however. While recoiling, the drops on the surfaces without wettability patterns [Figs. 3(a) and 3(b)] maintain axisymmetrical shapes, although the amount of retraction differs due to their differing affinities to water. When the surface is patterned such that hydrophilic spokes radiate on the hydrophobic background, as shown in Fig. 3(c), the recoiling drop leaves liquid along the thin lanes while retracting itself only on the

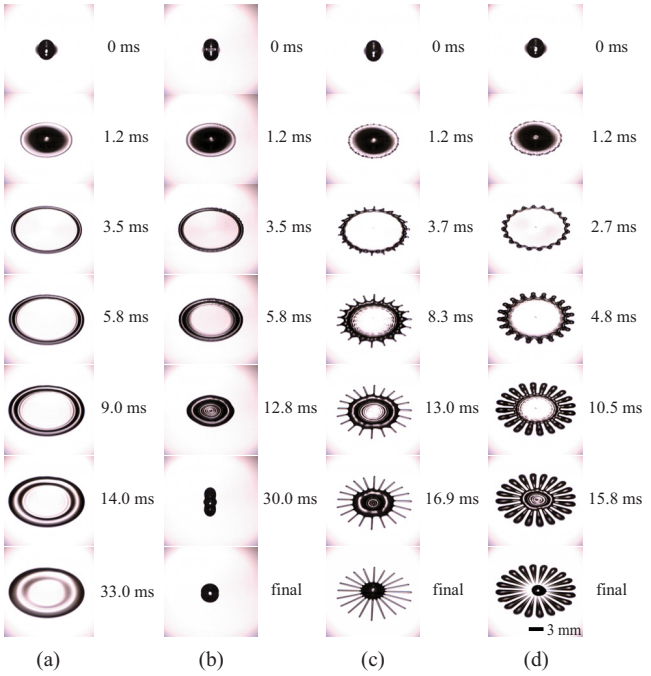

FIG. 3. (Color online) High-speed images of an impacting water drop on various surfaces: (a) piranha cleaned glass, (b) silane SAM surface, (c) surface with hydrophilic radiating arms resulted from the mask in Fig. 2(a), and (d) surface with hydrophobic radiating arms resulted from the mask in Fig. 2(b).

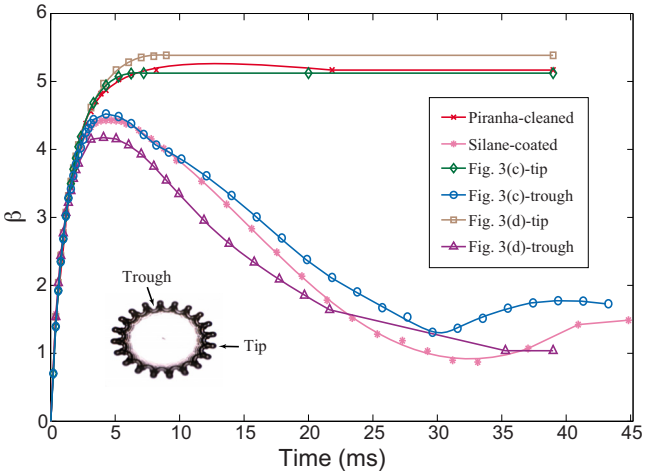

FIG. 4. (Color online) Temporal evolution of spreading degrees of the drops whose images are shown in Fig. 3.

nonwetting region. The consequence is a blob at the center with radiating threads exactly reproducing the photomask pattern. In this scenario, microscale liquid threads are formed, which are stable without exhibiting capillary beading instability[25,26] owing to the low contact angle of the hydrophilic region.[27] On the surface with hydrophobic spokes as in Fig. 3(d), the drop retracts only along the nonwetting lanes, leaving a great portion of its volume on the hydrophilic background which resembles the cross section of an orange. Although the original pattern has a central spot that tends to repel water, the recoiling inertia that has survived viscous dissipation gathers a small amount of liquid at the center.

A natural measure of how much spreading occurs is the spreading degree β defined as $\beta=R_c/R$, where R_c is the instantaneous contact radius. The dynamical evolution of β for those drops in Fig. 3 is shown in Fig. 4. All the drops spread with nearly identical speed in the initial spreading stages, regardless of the substrate wettability due to the dominance of inertia over capillarity. On surfaces with homogeneous wettability, the behavior of a drop can be adequately described by measuring only the parameter β as a function of time due to its axisymmetry. After reaching its maximum extent of spreading, the drop impacting on the hydrophobic silane SAM surface recoils, while that on a hydrophilic glass surface remains stationary. The maximum spreading degree defined as $\beta_{max}=R_{max}/R$, with R_{max} being the maximum spreading radius, is higher on the wetting glass surface ($\beta_{max}=5.2$) than that on the nonwetting SAM-coated surface ($\beta_{max}=4.4$). This is consistent with a similar observation in a previous study.[7] On wettability-patterned surfaces, the liquid behaviors on hydrophilic and hydrophobic regions differ within a single drop. Thus, two values of β should be used to describe the drop morphology evolution. We therefore measure the radial distance of both the tip and the trough, as defined in the inset of Fig. 4. Figure 4 shows the evolution of these values of β for the drops of Figs. 3(c) and 3(d). The results show that in the initial spreading stages the values of β for the tips and the troughs are indiscernible from those on the surfaces with uniform wettability. This is due to dominant inertial effects. However, the contact radii bifurcate as the drop approaches its maximum degree of spreading. For the drop of Fig. 3(c), the liquid on the hydrophobic regions (troughs) begins to recoil upon reaching only $\beta_{max}=4.5$, while the liquid on the hydrophilic spokes (tips) spreads further to $\beta_{max}=5.1$. At this point, the contact radius is kept constant like that of a drop on the uniformly wettable surface. The rate of recoiling of the troughs is not much different from that of a drop on the uniformly hydrophobic surface, although a slight decrease of the rate is observed presumably due to resistance by the immobile liquid threads on the hydrophilic spokes. On the surface with hydrophobic spokes [Fig. 3(d)], a similar bifurcation of β occurs between the tips and the troughs. Now the hydrophilic regions are broader than the hydrophobic spokes, and this appears to help the tips spread further ($\beta_{max}=5.4$) than is observed for the same drop on the other wettable surface of Fig. 3(a) and the tips on the hydrophilic spokes of Fig. 3(c). The tendency of β_{max} to increase with the widening of the hydrophilic regions is observed for other cases as will be discussed below. The troughs consequently spread less to reach only $\beta_{max}=4.2$. The tips become immobile and the troughs recoil after reaching their maximum spreading degrees like those in Fig. 3(c).

We varied the number of spokes (n) in our photomasks from 2 to 48 and their width (w) from 100 to 1000 μm. This enabled us to investigate the effect of these two parameters on the drop impact dynamics and also the shape of the final deposit. As shown in Fig. 5, all the wettablity patterns are successfully disclosed by the recoiling drop. In particular, we see that on the surfaces with hydrophobic spokes, the volume

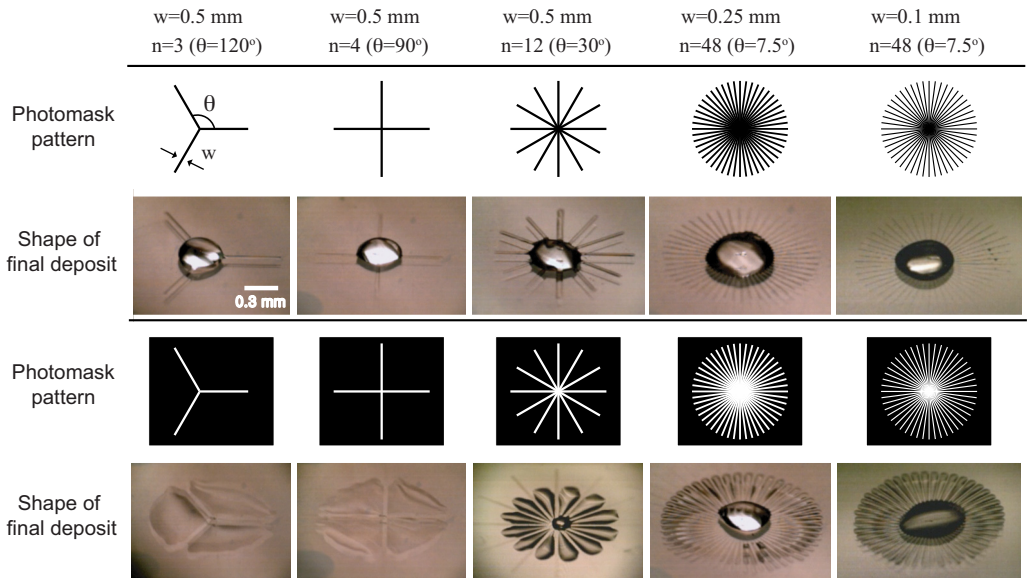

FIG. 5. (Color online) Images of final deposits obtained by the impacts of drops on the surfaces that are wettability-patterned with different numbers and widths of spokes.

of the central blob in the final deposit increases with the number of spokes, owing to the increase of the recoiling inertia (with the increase of hydrophobic area) that gathers liquid toward the center. Since the number and the width of spokes affect the maximum spreading degrees also, we experimentally measured the dependency of β_{max} on n and w at varying We. Figure 6 shows that, not surprisingly, β_{max} increases with the impact Weber number in all the cases. As Figs. 6(a) and 6(b) show, the values of β_{max} of both the tips and the troughs decrease as n increases, whether they are hydrophilic or hydrophobic. This is believed to be because

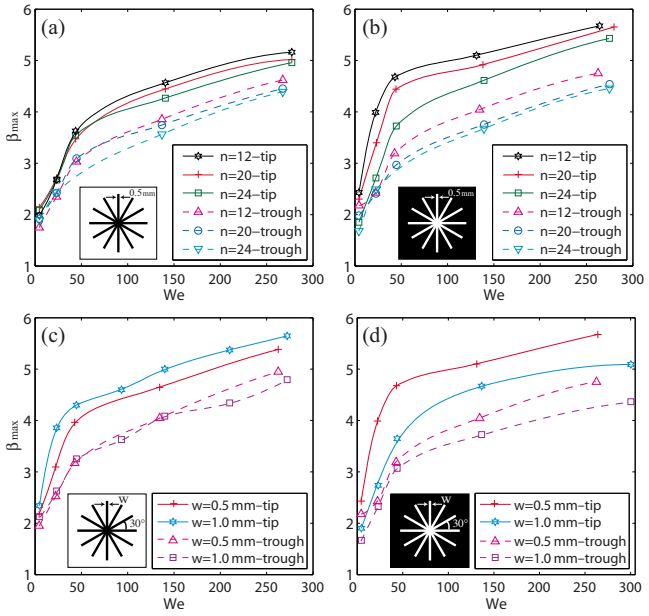

FIG. 6. (Color online) Dependency of the maximum spreading degrees on the number and width of spokes. Effects of varying (a) n of hydrophilic spokes, (b) n of hydrophobic spokes, (c) w of hydrophilic spokes, and (d) w of hydrophobic spokes at various We. w is fixed to be 500 μm for (a) and (b), and n is fixed to be 12 for (c) and (d).

the amount of liquid in each unit area (either a straight spoke or a triangular area between the neighboring spokes) decreases with the increase of the number of spokes, thereby reducing the inertia to drive the liquid outward. As w increases from 0.5 to 1 mm, while n is kept constant, the value of β_{max} for the tips increases [see Fig. 6(c)]. The increase of the amount of liquid on the widened hydrophilic spokes leads to the increase of β_{max} due to increased spreading inertia. This is consistent with the aforementioned trend that the drop impacting on the surface with hydrophobic spokes [Fig. 3(d)] spreads its tips more than it would on the surface with hydrophilic spokes (thus narrower wettable regions) [Fig. 3(c)]. When the hydrophobic spokes are widened as in Fig. 6(d), the spreading of the troughs on those spokes is not enhanced probably due to the suppressed spreading of neighboring tips on narrowed hydrophilic triangular regions. To understand quantitatively the detailed spreading behavior on microscale wetting patterns as experimentally observed in this work would require substantial numerical analysis, which is not pursued here.

B. Fingering instability

Although the effects of the radial wettability patterns manifest themselves most obviously in the recoiling stage described already, the patterns also induce corrugations of the rims in the spreading stages. This may be observed in the second and third frames of Figs. 3(c) and 3(d). The rims of spreading drops formed by impact of a drop onto a solid surface at high We are known to develop an instability, which is termed fingering. This fingering is observed even on smooth surfaces with uniform wettability when the impact inertia is sufficiently large.[12,28] It was proposed in Ref. 11 and experimentally verified in Ref. 29 that the fingering is caused by the Rayleigh–Taylor instability because a heavier fluid (liquid rim) is decelerated with respect to a lighter one (air) during spreading. The magnitude of the initial decelera-

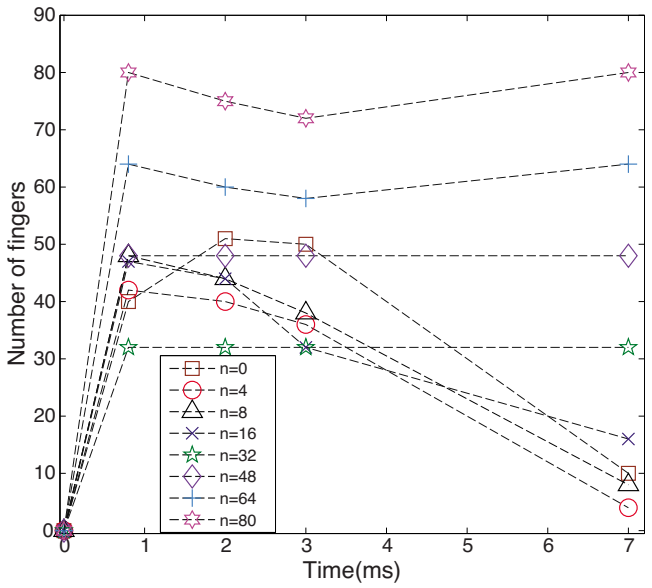

FIG. 7. (Color online) Temporal evolution of the number of fingers (f) during spreading and recoiling of drops with the impact Weber number of 172 on the surfaces with different numbers of hydrophilic spokes (n).

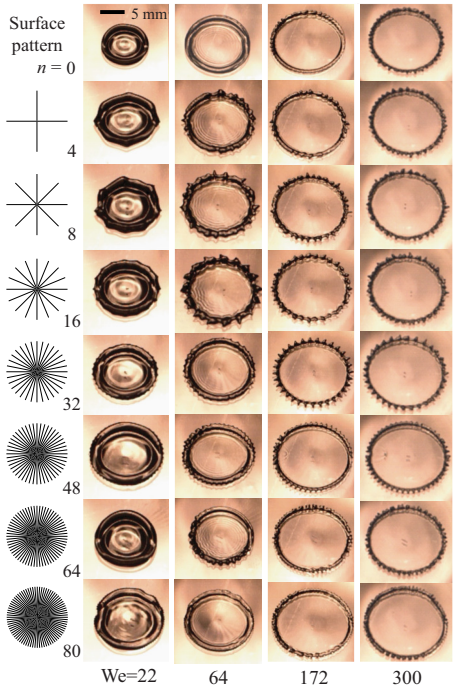

FIG. 8. (Color online) Images of drops impacting with various We on surfaces with various numbers of hydrophilic spokes at the maximum extent of spreading.

tion determines the number of fingers occurring in the very early stages of spreading, but the fingers can interact with each other to merge or split as the rim expands.[28] Here we investigate how the fingering instability that arises naturally on a surface of uniform wettability is affected by the radial wettability patterns introduced here.

We use a surface uniformly covered with the hydrophobic silane SAM to measure the number of fingers f that occur naturally without being affected by any wettability patterns. We then measure the numbers of fingers formed by collision with the surfaces with wettability patterns having differing numbers of hydrophilic spokes on the hydrophobic background. First we vary the number of spokes, keeping both the spoke width and impact We fixed ($w=500$ μm and We=172). We then measure the temporal evolution of the number of fingers for each surface. The results are shown in Fig. 7. On the surfaces with a small n, 0–16, more fingers than patterned spokes appear in the initial spreading stages (1–3 ms), then the number of fingers reduces to the value that exactly matches the number of the patterned spokes while recoiling (7 ms). For the surfaces with a moderate n, 32–48, the number of initially appearing fingers exactly matches that of the spokes and is kept constant throughout the drop spreading and recoiling processes. For the surfaces with a higher n, 64–80, the number of initially appearing fingers matches that of spokes as before, but the fingers tend to merge in the course of spreading, thus their number slightly decreases until time reaches 3 ms. The merging of fingers can be understood by considering the capillary pressure between the tip and the trough. The tips, besides being the protruding portions of the rim, are thicker than the troughs, thus the combined geometrical effects yield a Laplace pressure that is higher than that in the troughs. Then the flows tend toward troughs, leading to the merging of the fingers. In the recoiling stages, which are dominated by the hydrophobic nature of the regions between the spokes, the liquid is arrested precisely on the hydrophilic spokes thus the number of fingers matches that of spokes.

Figure 8 shows the images of the drops at their maximum extents of spreading to highlight the effects of the wettability patterns on the fingering instability for varying n and We. Figure 9(a) plots the number of fingers (f) in those images versus We for surfaces with varying number of spokes (n). When the impact We is low, 22, fingers are hardly seen on the surface with no wettability pattern ($n=0$) but are clearly visible on the surfaces with small and moderate numbers of hydrophilic spokes ($n=4-48$). When the number of spokes further increases ($n=64$ and 80), the fingers again disappear for this low We. On a surface with uniform wettability, the fingers emerge and their numbers increase as We increases, as predicted by the established theory.[11] The same tendency for the number of fingers to increase with We can be found for the surfaces with small n up to 16 and with very high n (64 and 80). However, such an increase of the number of fingers is seen to saturate as We exceeds 172. For the surfaces with a moderate number of spokes ($n=32$ and 48), the number of fingers is constant and is equal to the number of spokes throughout the range of We tested in this work.

Rearranging the measurement data, as shown in Fig. 9(b), clarifies the subtle dependency of the number of fingers (f) on n and We. In this figure, the abscissa corresponds to the number of patterned spokes n and the ordinate to the number of observed fingers f. The straight line designates the cases when $f=n$. The points for $n=0$, i.e., on the y-axis, correspond to the number of fingers occurring on the surface with the uniform wettability for each We. For the surfaces of small n, region I, the measurement points lie above the

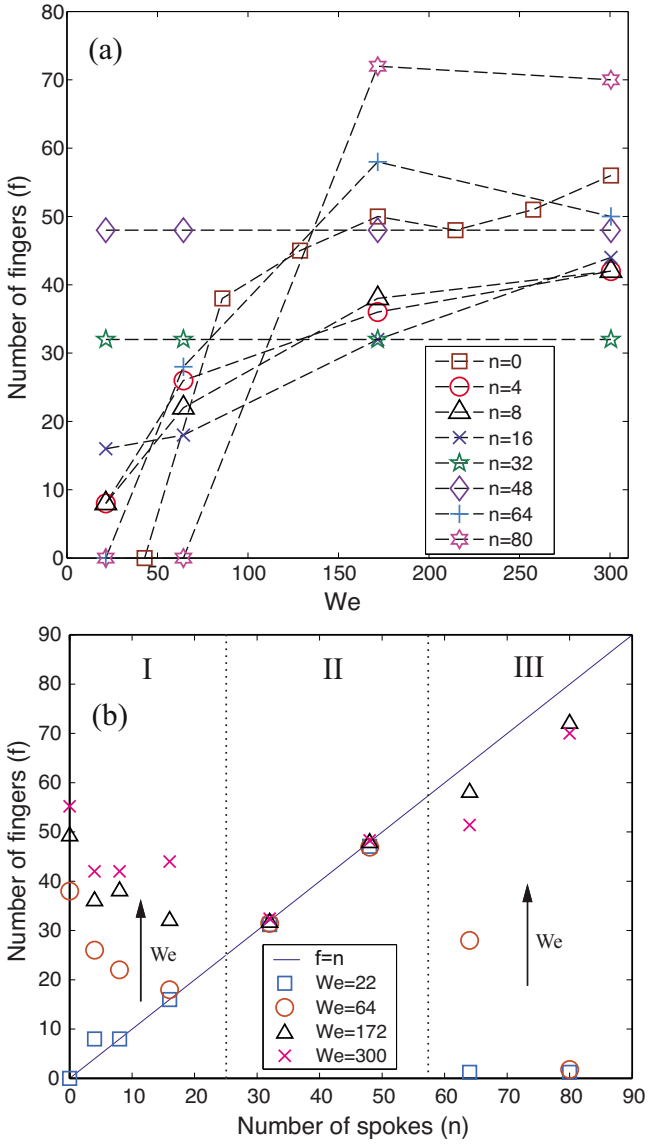

FIG. 9. (Color online) Dependency of the number of fingers on the Weber number and the number of hydrophilic spokes. (a) f vs We on the surfaces with different n. (b) f vs n for drops with different We. Three distinct regimes appear depending on n.

straight line ($f>n$), thus it can be stated that the fingering formation is driven by the natural instability rather than the externally imposed wettability patterns. Such a tendency is particularly pronounced for high values of We (172 and 300) in region I: f is hardly affected by n at large We. For the surfaces of moderate n, region II, we see that $f=n$ throughout the entire range of We tested. In this region, the number of naturally occurring fingers is close to n and so the intrinsic tendency to become unstable is consistent with the external perturbations due to wettability patterns. In region III, where the surfaces have large n, all the points lie below the straight line. The drop impacts with the lowest We (We=22 and 64) do not even develop fingers in the spreading stages due to a lack of inertia to give rise to such high curvature. As We increases, f tends to match n, which is higher than the number of naturally occurring fingers in the absence of patterning. Here we recall that the number of fingers is the same as the number of spokes for this high n in the very early stages of spreading as seen in Fig. 7. Thus, in region III, the fingering is governed by the externally imposed wettability patterns rather than the intrinsic rim instability.

IV. CONCLUSIONS

We have shown that the dynamics of a liquid drop impacting on a solid surface is greatly influenced by forming radial wettability patterns on the target surface. These effects are most pronounced in the recoiling stages where the contact lines recede on the hydrophobic regions while they are pinned on the hydrophilic regions. The resulting deposit shape is a central blob radiating either thin spokes or narrow fans. In addition, the wettability patterns have been shown to alter the stability of the spreading rim: the number of fingers appearing in the spreading stages is a subtle function of both the number of spokes and the impact Weber number. When the number of spokes is small ($n \leq 16$), the number of fingers tends to follow the number of naturally occurring fingers on the surface with uniform wettability rather than the number of spokes. In this regime the number of fingers therefore depends on We. For intermediate numbers of spokes (32 and 48), the number of spokes and that of fingers match throughout the drop spreading and recoiling stages. When the number of spokes is very high ($n \geq 64$), the number of fingers tends to follow the number of spokes, rather than the number of naturally occurring fingers, as We increases.

We believe that the transient shape evolution of the drops on the wettability-patterned surfaces as observed in this work poses a very interesting problem to be addressed computationally. We also believe that the intriguing shapes of the final deposits, obtained through the simple process of impact and subsequent recoiling of drops on microwetting patterned surfaces, could potentially be utilized in a variety of microfluidic applications. For instance, various functional liquids, e.g., biological or electrical, can be directly printed in microscales using the current drop impact method for such applications as DNA chips,[30] cell communication study,[31] and electric circuit printing.[32] It could also be of interest to reduce the width of the wettability patterns down to near nanometer scales to directly obtain nanoliquid threads. This could open a new pathway to simple and cheap creation of nanoliquid patterns.

ACKNOWLEDGMENTS

We are grateful to Dr. Dominic Vella for critically reading the manuscript. This work was supported by the National Research Foundation of Korea (Grant Nos. R01-2006-000-10444-0 and 412-J03001) and administered via SNU-IAMD.

[1] A. M. Worthington, "On the forms assumed by drops of liquid falling on a horizontal plate," Proc. R. Soc. London **25**, 262 (1877).
[2] M. Rein, "Phenomena of liquid drop impact on solid and liquid surfaces," Fluid Dyn. Res. **12**, 61 (1993).
[3] A. L. Yarin, "Drop impact dynamics: Splashing, spreading, receding, bouncing…," Annu. Rev. Fluid Mech. **38**, 159 (2006).
[4] H. Fukanuma, "A porosity formation and flattening model of an impinging molten particle in thermal spray coating," J. Therm. Spray Technol. **3**, 33 (1994).
[5] M. S. Sehmbey, M. R. Pais, and L. C. Chow, "Effect of surface material

properties and surface characteristics in evaporative spray cooling," J. Thermophys. Heat Transfer **6**, 505 (1992).
[6]Y.-S. Yang, H.-Y. Kim, and J.-H. Chun, "Spreading and solidification of a molten microdrop in the solder jet bumping process," IEEE Trans. Compon. Packag. Technol. **26**, 215 (2003).
[7]H.-Y. Kim and J.-H. Chun, "The recoiling of liquid droplets upon collision with solid surfaces," Phys. Fluids **13**, 643 (2001).
[8]R. Rioboo, M. Marengo, and C. Tropea, "Time evolution of liquid drop impact onto solid, dry surfaces," Exp. Fluids **33**, 112 (2002).
[9]H. J. Lee and H.-Y. Kim, "Control of drop rebound with solid target motion," Phys. Fluids **16**, 3715 (2004).
[10]D. Richard and D. Quéré, "Bouncing water drops," Europhys. Lett. **50**, 769 (2000).
[11]H.-Y. Kim, Z. C. Feng, and J.-H. Chun, "Instability of a liquid jet emerging from a droplet upon collision with a solid surface," Phys. Fluids **12**, 531 (2000).
[12]C. H. R. Mundo, M. Sommerfeld, and C. Tropea, "Droplet-wall collisions: Experimental studies of the deformation and breakup process," Int. J. Multiphase Flow **21**, 151 (1995).
[13]D. Richard, C. Clanet, and D. Quéré, "Contact time of a bouncing drop," Nature (London) **417**, 811 (2002).
[14]Z. Wang, C. Lopez, A. Hirsa, and N. Koratkar, "Impact dynamics and rebound of water droplets on superhydrophobic carbon nanotube arrays," Appl. Phys. Lett. **91**, 023105 (2007).
[15]J. Bico, C. Tordeux, and D. Quéré, "Rough wetting," Europhys. Lett. **55**, 214 (2001).
[16]Y. Chen, B. He, J. Lee, and N. A. Patankar, "Anisotropy in the wetting of rough surfaces," J. Colloid Interface Sci. **281**, 458 (2005).
[17]Y. Zhao, Q. Lu, M. Li, and X. Li, "Anisotropic wetting characteristics on submicrometer-scale periodic grooved surface," Langmuir **23**, 6212 (2007).
[18]V. Jokinen, L. Sainiemi, and S. Franssila, "Complex droplets on chemically modified silicon nanograss," Adv. Mater. (Weinheim, Ger.) **20**, 3453 (2008).
[19]D. Sivakumar, K. Katagiri, T. Sato, and H. Nishiyama, "Spreading behavior of an impacting drop on a structured rough surface," Phys. Fluids **17**, 100608 (2005).
[20]L. Xu, "Liquid drop splashing on smooth, rough, and textured surfaces," Phys. Rev. E **75**, 056316 (2007).
[21]R. Kannan and D. Sivakumar, "Drop impact process on a hydrophobic grooved surface," Colloids Surf., A **317**, 694 (2008).
[22]D. E. Kataoka and S. M. Troian, "Patterning liquid flow on the microscopic scale," Nature (London) **402**, 794 (1999).
[23]B. Zhao, J. S. Moore, and D. J. Beebe, "Surface-directed liquid flow inside microchannels," Science **291**, 1023 (2001).
[24]M. K. Chaudhury and G. M. Whitesides, "How to make water run uphill," Science **256**, 1539 (1992).
[25]S. H. Davis, "Moving contact lines and rivulet instabilities. Part 1. The static rivulet," J. Fluid Mech. **98**, 225 (1980).
[26]K. Sekimoto, R. Oguma, and K. Kawasaki, "Morphological stability analysis of partial wetting," Ann. Phys. **176**, 359 (1987).
[27]S. Schiaffino and A. A. Sonin, "Formation and stability of liquid and molten beads on a solid surface," J. Fluid Mech. **343**, 95 (1997).
[28]S. T. Thoroddsen and J. Sakakibara, "Evolution of the fingering pattern of an impacting drop," Phys. Fluids **10**, 1359 (1998).
[29]N. Z. Mehdizadeh, S. Chandra, and J. Mostaghimi, "Formation of fingers around the edges of a drop hitting a metal plate with high velocity," J. Fluid Mech. **510**, 353 (2004).
[30]C.-Y. Lee, S. Kamal-Bahl, H. Yu, J. W. Kwon, and E. S. Kim, "On-demand DNA synthesis on solid surfaces by four directional ejectors on a chip," J. Microelectromech. Syst. **16**, 1130 (2007).
[31]K. Shen, V. K. Thomas, M. L. Dustin, and L. C. Kam, "Micropatterning of costimulatory ligands enhances CD4$^+$T cell function," Proc. Natl. Acad. Sci. U.S.A. **105**, 7791 (2008).
[32]H. Sirringhaus, T. Kawase, R. H. Friend, T. Shimoda, M. Inbasekaran, W. Wu, and E. P. Woo, "High-resolution inkjet printing of all-polymer transistor circuits," Science **290**, 2123 (2000).